Measurement of dynamical dipole γ-ray emission in the N/Z-asymmetric fusion reaction $^{16}O + ^{116}Sn$ at 12 MeV/nucleon

A. Giaz,[1,*] A. Corsi,[1,†] S. Barlini,[6] V. L. Kravchuk,[3,‡] O. Wieland,[2] M. Colonna,[8] F. Camera,[1] A. Bracco,[1] R. Alba,[8] G. Baiocco,[5,§] L. Bardelli,[6] G. Benzoni,[2] M. Bini,[6] N. Blasi,[2] S. Brambilla,[2] M. Bruno,[5] G. Casini,[10] M. Ciemala,[4] M. Cinausero,[3] F. C. L. Crespi,[1] M. D'Agostino,[5] M. Degerlier,[3,‖] M. Di Toro,[9] F. Gramegna,[3] M. Kmiecik,[4] S. Leoni,[1] C. Maiolino,[8] A. Maj,[4] T. Marchi,[3] K. Mazurek,[4] S. Myalski,[4] B. Million,[2] D. Montanari,[1,¶] L. Morelli,[5] R. Nicolini,[1] G. Pasquali,[6] S. Piantelli,[10] A. Ordine,[7] G. Poggi,[6] V. Rizzi,[3] C. Rizzo,[8] S. Sambi,[5,**] D. Santonocito,[8] and V. Vandone[1]

[1]*Dipartimento di Fisica, Università di Milano and INFN sezione di Milano, via Celoria 16, 20133 Milano, Italy*

[2]*INFN sezione di. Milano, via Celoria 16, 20133 Milano, Italy*

[3]*Istituto Nazionale di Fisica Nucleare, Laboratori Nazionali di Legnaro, Legnaro, Italy*

[4]*The Henryk Niewodniczański Institute of Nuclear Physics, PAN, 31-342, Krakow, Poland*

[5]*Dipartimento di Fisica ed Astronomia, Università di Bologna and INFN sezione di Bologna, Bologna, Italy*

[6]*Dipartimento di Fisica, Università di Firenze and INFN sezione di Firenze, Firenze, Italy*

[7]*INFN sezione di Napoli, Napoli, Italy*

[8]*Istituto Nazionale di Fisica Nucleare, Laboratori Nazionali del Sud, Catania, Italy*

[9]*Dipartimento di Fisica e Astronomia dell'Università di Catania and Istituto Nazionale di Fisica Nucleare, Laboratori Nazionali del Sud, Catania, Italy*

[10]*INFN sezione di Firenze, Firenze, Italy*

(Received 24 January 2014; revised manuscript received 3 June 2014; published 18 July 2014)

A new measurement of the dynamical dipole emission was performed in the system $^{16}O + ^{116}Sn$ at 12 MeV/nucleon. These data, together with those measured at 8.1 MeV/nucleon and 15.6 MeV/nucleon on the same system, provide the dependence of the dynamical dipole total emission yield on the beam energy. The energy removed by preequilibrium charged particles emission was directly measured and this made possible the direct estimation of the compound nucleus excitation energy. The experimental results show a weak increase of the dynamical dipole total yield with beam energy and they are in agreement both in trend and in absolute values with the predictions of the theoretical model based on the Boltzmann-Nordheim-Vlasov approach. The measured γ-ray angular distribution has a dipole character but with a strong quenching probably owing to the rotation of the dipolar axis during the fusion and thermalization processes.

DOI: 10.1103/PhysRevC.90.014609 PACS number(s): 24.30.Cz, 25.70.Gh

I. INTRODUCTION

In heavy-ion fusion reactions, if the N/Z ratio between projectile and target nuclei is different, a N/Z equilibration process takes place. The related neutron-proton motion has the feature of a collective oscillation and it is associated with a γ emission, the so-called dynamical dipole (DD) emission. The total intensity yield of such emission depends on the fusion dynamics and, in particular, on the symmetry term of the equation of state (EOS) [1]. This parameter attracts much interest in the scientific community because of its implications beyond nuclear dynamics, namely neutron stars or supernovae burning [2–8]. The sensitivity to the symmetry term of the EOS is expected to be larger in reactions with exotic radioactive beams. However, this work shows that, under selected experimental conditions, a good sensitivity is expected also using stable beams.

The DD was predicted theoretically some years ago for heavy-ion collisions as a collective mode in the fusion process [6–12]. Its experimental evidence was found in both fusion-evaporation and deep-inelastic reactions [13–20]. This phenomenon is expected to depend both on the energy of the projectile and on the size of the "static" dipole moment $D(0)$. The latter is defined as

$$D(0) = \frac{r_0\left(A_p^{1/3} + A_t^{1/3}\right)}{A} Z_p Z_t \left|\frac{N_t}{Z_t} - \frac{N_p}{Z_p}\right|, \qquad (1)$$

where $r_0 = 1.2$ fm, and the indexes p and t refer to the projectile and the target of the reaction, respectively. In principle, one could expect the DD total yield to increase with $D(0)$. In fact, for a fixed compound nucleus (CN), as the N/Z asymmetry between projectile and target increases; i.e., as $D(0)$ increases, the charge flow in the fusion process becomes larger, leading to a stronger total DD emission yield [21]. From the experimental point of view, however, data [17,18] do not clearly confirm the expected scenario. Moreover, the very few data available come from different experimental setups, use different experimental

*agnese.giaz@mi.infn.it

†Present address: CEA, Centre de Saclay, IRFU/Service de Physique Nucléaire, 91191 Gif-Sur-Yvette, France.

‡Present address: Kurchatov Institute, Moscow, Russia.

§Present address: Dipartimento di fisica, Università di Pavia and INFN Sezione di Pavia.

‖Present address: Physics Department, Nevsehir University, Turkey.

¶Present address: Institut d'Etudes Avancées de l'Université de Strasbourg and Institut Pluridisciplinaire Hubert Curien, CNRS, Strasbourg, France.

**Present address: Katholieke Universiteit Leuven, Belgium.

techniques, and have large error bars. A systematic and detailed study on the $D(0)$ dependence would require the measurement of the DD total emission yield in the same fused CN using different projectile/target combinations with different N/Z asymmetries. This will be possible only with the availability of intense low-energy radioactive beams, namely with new facilities as SPES [22] or SPIRAL2 [23].

It is possible anyway to study the dependence of the DD total yield on the beam energy with the presently available stable heavy-ion beam facilities. Theoretically, one expects that the DD emission develops mainly in the neck region between projectile and target. As the dipole acceleration increases with the beam energy, the DD emission should be enhanced [21]. However, for high beam energies, the damping related to fast processes like preequilibrium particles emission and nucleon-nucleon direct collisions is expected to reduce the N/Z asymmetry and the DD total yield. Experimentally, the only data available, at different beam energies, at the moment on DD total emission concern the fused compound ^{132}Ce nucleus. In the work reported in Ref. [24], ^{132}Ce was formed via different reactions characterized by $D(0) =$ 18–21 fm. The DD was observed to rise approximately by a factor six as the beam energy increases from 6 to 9 MeV/nucleon and then to decrease by a factor two from 9 to 16 MeV/nucleon. Such a steep "rise-and-fall" trend, however, cannot be reproduced by model calculations based on the Boltzmann-Nordheim-Vlasov approach (BNV), which predict a continuous but weak increase of the total yield for the beam energy window 6–16 MeV/nucleon. This disagreement still constitutes a puzzling open problem.

The same CN was studied by Corsi *et al.* [18], using the same reaction, namely ^{16}O + ^{116}Sn, at two different beam energies, 8.1 and 15.6 MeV/nucleon. In this case, $D(0)$ is equal to 8.6 fm. With only two points, however, nothing can be said about the presence of the rise-and-fall trend observed in Ref. [24].

In this work, we measured the DD total yield in the CN ^{132}Ce via the reaction ^{16}O + ^{116}Sn at 12 MeV/nucleon. Together with the data of Ref. [18], our results provide a complete beam energy dependence in the range 8.1–15.6 MeV/nucleon and constitute a second and important test for the trend of the DD and the predictions of theoretical models.

In the next section the two experimental techniques used to extract the DD total yield are discussed. The experimental setup is described in Sec. II. Section III discusses the measurement of the energy removed by preequilibrium particles. This is a critical input to estimate the CN evaporation emission obtained from statistical model calculations that has to be subtracted from the experimental data to deduce the DD total yield (discussed in Sec. IV). The comparison between the experimental data and model predictions is presented in Sec. V. Finally, the measured γ angular distribution is discussed and compared with theory in Sec. VI.

The measurement technique

The γ rays from the preequilibrium DD emission lie in the energy region between 10 and 22 MeV. In the same region, one observes the statistical γ decay of the giant dipole resonance (GDR) from the thermally equilibrated compound nuclei, which has a dipole nature as the DD γ-ray emission.

Experimentally, the previously measured DD total yield was extracted using two different techniques [18,24]. Both techniques require the measurement of the high-energy γ-ray emission from the same CN formed by two different reactions. In one reaction the target-projectile combination is N/Z asymmetric. In this case, both the DD and hot GDR emissions are expected to be present in the energy range of 10–22 MeV. The second reaction uses a N/Z symmetric target-projectile combination and it is used as a "reference" case. It produces an equal or similar CN at a very close excitation energy and angular momentum as in the asymmetric reaction, but in this case only the hot GDR contribution is expected to be present.

The techniques used to extract the DD yield in Refs. [18] and [24] differ in the way the reference high-energy γ-ray spectrum is used. In Ref. [24], the measured reference spectrum is subtracted from the asymmetric system spectrum. This can be done only if the two compound nuclei are produced at identical excitation energy and angular momentum distribution; otherwise, a systematic error in the DD total yield value might arise. Therefore, the preequilibrium particle emission, the compound angular momentum and the excitation energy should be estimated *a priori* to choose the proper beam energy and then verified experimentally during the data analysis.

In the technique used in Ref. [18], the reference high-energy γ-ray spectrum was reproduced by the statistical model (which does not include DD emission). Then, the statistical model was used to calculate the high-energy γ-ray spectrum emitted in the N/Z asymmetric fusion-evaporation reaction using the same statistical and GDR parameters as for the reference case. The difference between the measured γ-ray spectrum in the N/Z asymmetric reaction and the calculated one provides the DD total emission. Because this technique requires the knowledge of the preequilibrium energy loss owing to particle emission, the emitted particles should be measured. Because the reference spectrum is only used for tuning the calculations, the CN mass A, the atomic number, the angular momentum, and the excitation energy do not need to be exactly the same for the symmetric and asymmetric reactions, unlike in the case of Ref. [24]. In this work, this latter technique is used.

II. EXPERIMENTAL SETUP

The experiment was performed using the ALPI accelerator of the Laboratori Nazionali di Legnaro. The reaction ^{16}O + ^{116}Sn $\Rightarrow$ ^{132}Ce* at 12 MeV/nucleon was produced. The target of ^{116}Sn was 0.5 mg/cm^2 thick. The experimental setup used for this experiment is the GARFIELD-HECTOR apparatus (very similar to the one used in Ref. [18]), which can measure high-energy γ rays, light-charged particles (LCPs) and evaporation residues.

The Hector array [25] consists of eight large-volume (approximately 14 $\times$ 18 cm) BaF_2 crystals used to measure high-energy γ-rays. The Garfield array [26] consists of ΔE-E gaseous microstrips and CsI(Tl) scintillation detectors lodged in the same gas volume for the measurement of LCP. The evaporated residues are detected in a wall of 32 Phoswich detectors from the Fiasco array [27] placed at forward

angles. These Phoswich detectors consist of three different scintillation detectors: two organic scintillators and a CsI(Tl). Both the Garfield array and the Phoswich detectors use newly developed digital electronics [28,29]. The experimental setup was located inside the Garfield scattering chamber (a cylinder of ~3 m diameter and 5 m length). All detectors operated in vacuum ($\sim 10^{-5}$ mbar).

The calibrations of the Garfield detectors were performed during dedicated measurements before the experiment. As a normalization point, the elastically scattered beam on a gold target was used during the present measurement. This calibration and periodic checks performed during the experiment allowed to control and correct for any possible gain shift owing to electronics. The BaF_2 detectors were calibrated using standard γ-ray sources and the 15.1-MeV γ rays from the reaction $d(^{11}B,n\gamma)^{12}C$ at beam energy of 19.1 MeV. The intrinsic time resolution of BaF_2 (less than 1 ns) allowed the background and neutron rejection by time-of-flight (ToF) measurement. An electronic threshold of ~3 MeV was set on the γ-ray energies to reduce the acquisition dead time.

The trigger conditions consisted in the requirement of a coincidence of signals between high-energy γ-rays and fusion-evaporation residues. In addition, scaled down counts from the Phoswich, Garfield, and Hector detectors in single mode were registered. In the analysis of the particle and γ-ray data an appropriate gate on the ToF vs energy loss in the first scintillator layer of the Phoswich detector was set (indicated by a black circle in Fig. 1) to select the fusion-evaporation residues. A further condition on the BaF_2 ToF parameter made it possible to better select the γ rays coming from the target.

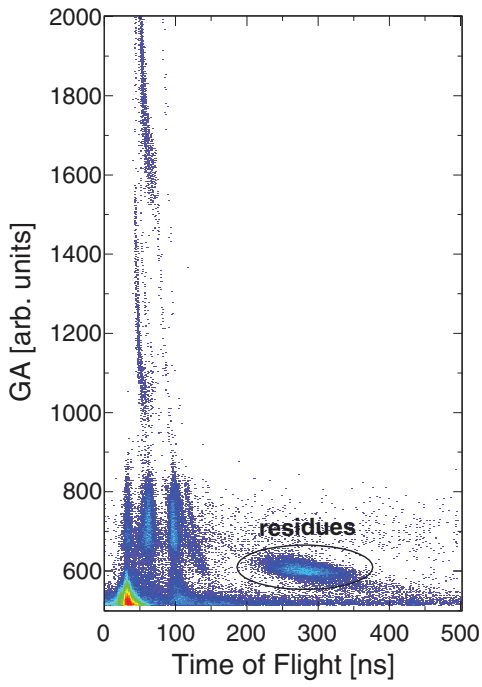

FIG. 1. (Color online) The measured Phoswich ToF vs deposited energy in the first scintillator layer of the Phoswich detectors (indicated as GA). The black circle is the gate used to select the evaporation residues. The matrix has the requirement of a coincident high-energy γ ray ($E > 5$ MeV).

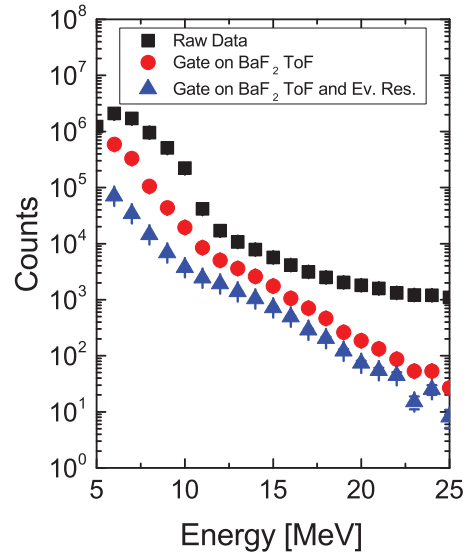

FIG. 2. (Color online) The measured high-energy γ-ray spectra for the system $^{16}O + ^{116}Sn$ at 12 MeV/nucleon without (black squares) and with the experimental conditions on γ ToF (red dots) and ToF and residues (blue triangles).

Figure 2 shows the measured high-energy γ-ray spectra before and after applying the experimental selection gates. The ToF gate on BaF_2 removes neutrons (i.e., the "bump" between 5 and 10 MeV), background, and cosmic-rays events, while the gate on residues selects the reaction channel removing contaminations from other channels like, for example, fission.

The bremsstrahlung contribution, which can be estimated from events at energy higher than 23–25 MeV contributes to the total integral 10–22 MeV yield for less than 10%.

III. PREEQUILIBRIUM PARTICLE EMISSION

In the reaction $^{16}O + ^{116}Sn$, the charged particle energy spectra measured in coincidence with the evaporation residues show the presence of preequilibrium particle emission. The spectra of proton and α particles measured at various polar angles are shown in Fig. 3.

It is important to stress that such LCP preequilibrium emission is not related to the DD mechanism discussed in the Introduction. In fact, its origin is not related to isospin effects in the entrance channel of the reaction but simply to the high projectile velocity, as discussed in Refs. [30–33]. When preequilibrium particle emission occurs, the final excitation energy of the compound system is lower than the expected one for a complete fusion reaction, because the fast emitted particles take part of the energy away. Therefore, it is very important to take the amount of removed energy into proper account, because it affects the results of the total DD yield.

Because no accurate prediction on the preequilibrium particle emission energy loss can be provided by theory, this should be measured experimentally. In this work, the preequilibrium energy loss was deduced from the analysis of the light charged particle energy spectra measured in the

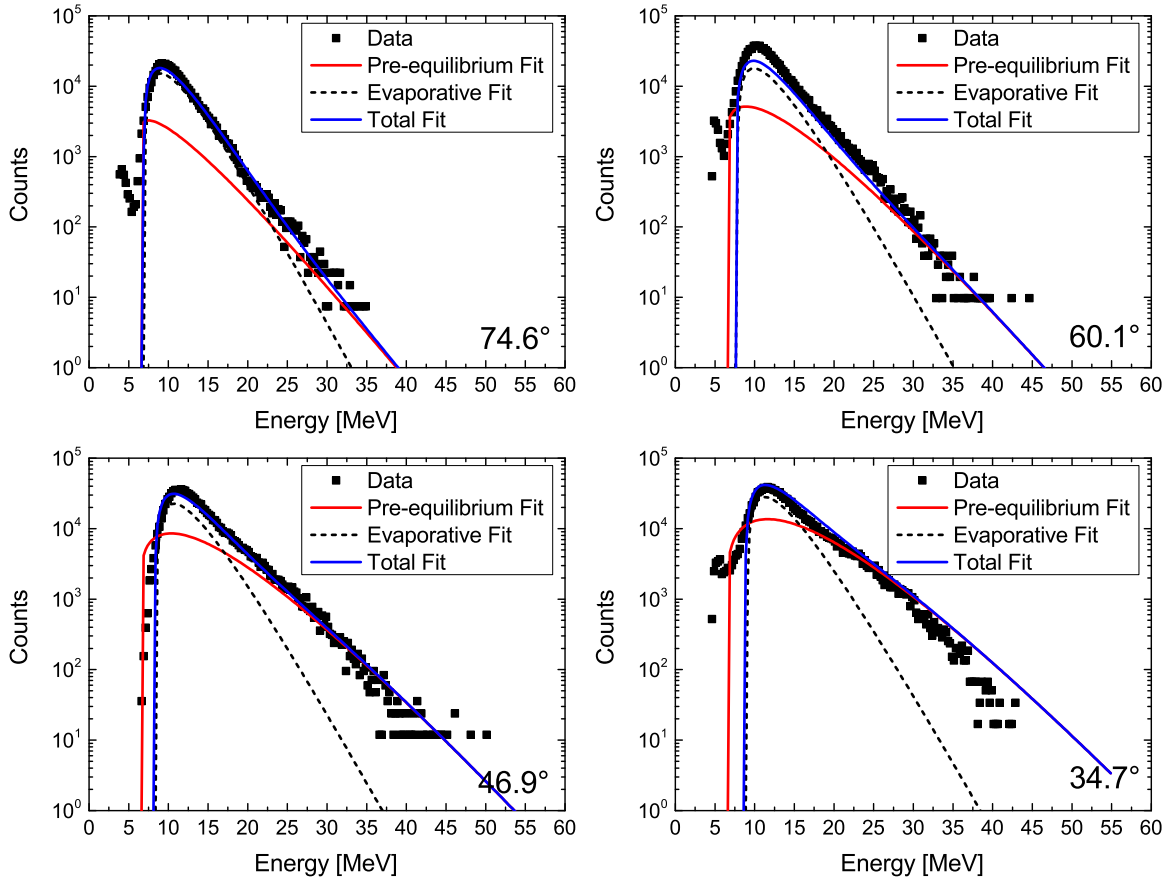

FIG. 3. (Color online) The α-particle energy spectra measured at different angles by the Garfield array. The continuous blue line indicates the results of a moving source fit, where the spectra are fitted by a combination of two distributions: The first one (continuous red line) describes the pre-equilibrium emission, while the second one (dashed black line) describes the particle statistical emission.

Garfield array, using the expression

$$E_{\rm loss} = (K_p + B_p)\, M_p^{\rm PE} + (K_\alpha + B_\alpha) M_\alpha^{\rm PE} + (K_n + B_n) M_n^{\rm PE}, \quad (2)$$

where K is the kinetic energy, B represents the binding energy, and $M^{\rm PE}$ is the preequilibrium multiplicity. The subscripts p, α, and n stand for proton, α particle, and neutron, respectively.

This procedure was already applied in Ref. [18]. The experimental charged particle energy spectra were reproduced by a moving source fit [34] including the two contributions of the statistical and the preequilibrium particle emission. The velocities of the thermalized source extracted from the fit procedure is 0.58 cm/ns (α particles and proton energy spectra fit give the same value). The "preequilibrium" source extracted from the fit is 2.7 cm/ns for protons and 2.0 cm/ns for α particles. The velocity of the thermalized source is the same of that of the CN, while the velocity of the preequilibrium source is intermediate between that of compound and that of the projectile (4.8 cm/ns). The preequilibrium contribution, in the fit, was based on the Watt distribution [35], successfully applied in previous works (see, e.g., [30–32]). The preequilibrium neutron multiplicity was instead estimated using the theoretical model reported in Ref. [36]. As an additional cross check, we compared the neutron multiplicity predicted by this model with the values available in the literature [30], as shown in Fig. 4. As can be seen, the calculated multiplicities are consistent with the experimental data within the errors.

The estimated energy losses owing to preequilibrium emission are listed in Table I for proton, neutron, and α particles.

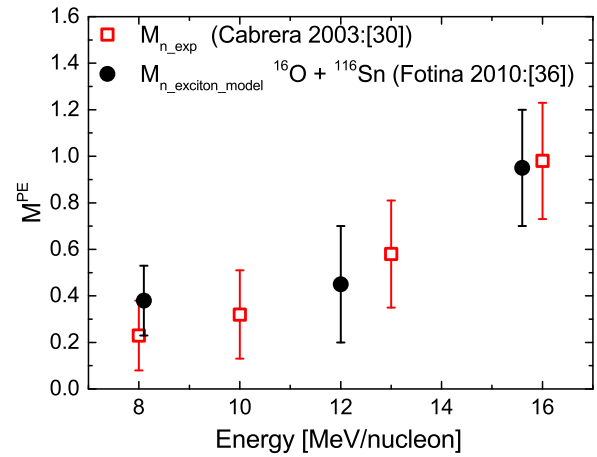

FIG. 4. (Color online) The neutron preequilibrium multiplicity obtained from the model of Ref. [36] for the same reaction at different beam energies (black points) is compared to the data available in literature [30] (red squares).

TABLE I. The second column reports the values of the preequilibrium multiplicities extracted from data for protons and α particles and from model for neutrons. The third column lists the values of the average kinetic energy of the emitted particles. The last column shows the contribution in the calculation of energy removed by preequilibrium particle emission. Note that E loss is not the product between $\langle E_{\rm kin}\rangle$ and the multiplicity as the reaction Q values has to be considered.

Emitted particle	Preequilibrium multiplicity	$\langle E_{\rm kin}\rangle$ (MeV)	E loss (MeV)
Neutrons	0.45	4.3	6.8
Protons	0.18	14.8	3.7
α particles	0.13	21.7	2.8
Total			13.3

The total energy removed from preequilibrium emission is 13.3 $\pm$ 2.5 MeV. In the evaluation of the error bars, the uncertainties coming from the theoretical model [36] for neutrons had a predominant weight relative to the error coming from the moving source fit procedure on the Garfield spectra for α particles and protons (see Fig. 3).

The energy loss measured for 12 MeV/nucleon is consistent with the values reported in Ref. [30,37]. This value is smaller than the one obtainable from the parametrization of Kelly *et al.* [38], who, however, did not measure it directly, but used a linear interpolation between two measured points for the reaction ^{18}O + ^{100}Mo. Once reconstructed, the energy removed by preequilibrium particles, it was possible to estimate that the excitation energy of the CN was $E^* = 142$ MeV.

IV. STATISTICAL MODEL CALCULATIONS

As discussed in the previous sections, the statistical γ decay of the GDR and the DD pre-equilibrium emission have a very similar energy interval and the same dipolar nature. To disentangle the DD emission one has to estimate the statistical γ-ray spectrum and then subtract it to the measured one. The signature of a DD emission is an excess of events, relative to the "pure statistical" ones, in the energy region 10–22 MeV.

We performed statistical model calculations adjusting the parameters to reproduce the γ-ray spectra measured in the reaction ^{64}Ni + ^{68}Zn at 300 (4.7 MeV/nucleon), 400 (6.3 MeV/nucleon), and 500 MeV (7.8 MeV/nucleon), as discussed in Refs. [18,39]. Because the N/Z ratio in this reaction is symmetric, no significant DD emission is expected. Furthermore, owing to the low beam energy per nucleon, the preequilibrium particle emission is very small.

For the reaction ^{16}O + ^{116}Sn at 12 MeV/nucleon, the CN excitation energy is $E^* = 142$ MeV. A smoothed triangular spin distribution (extracted from Refs. [18,39] and from statistical model cross section) with vertex at $J = 58\ \hbar$, $\langle J\rangle = 42\ \hbar$, and the inflection point at $J_{\rm flex} = 63\ \hbar$ was used. The GDR was parametrized with a single Lorentzian strength function centered at $E_{\rm GDR} = 14$ MeV and a value of the energy-weighted sum rule corresponding to 100% of the Thomas-Reiche-Kuhn sum rule. The used GDR width was also extracted from the parametrization of Ref. [39],

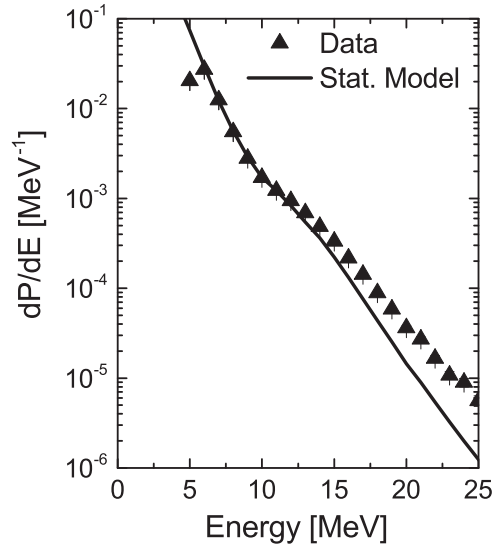

FIG. 5. The comparison between the total spectrum (triangles) measured in the reaction ^{16}O + ^{116}Sn at 12 MeV/nucleon and the corresponding statistical model calculations (line). The calculations were folded with the detector response function and normalized at 7–8 MeV.

namely, 10.2 MeV. The level density description was the Reisdorf formalism of Ignatyuk [40,41]. The calculations were folded with the response function of the BaF_2 array calculated using the GEANT [42] libraries. Data and statistical model calculations were normalized in the region 7–8 MeV.

Figure 5 shows the measured high-energy γ-ray spectrum, measured in the reaction ^{16}O + ^{116}Sn at 12 MeV/nucleon, compared to the corresponding statistical model calculations. As expected, an excess of γ rays in the energy region between 10 and 22 MeV is observed.

The energy loss of 13.3 $\pm$ 2.5 MeV was used to deduce the value of the DD yield at 12 MeV/nucleon, which is compared to the values measured at 8.1 and 15.6 MeV/nucleon [18] in Table II. The error bars of the DD total emission yield are mainly attributable to the uncertainty in the estimation of the value of the preequilibrium energy loss.

It can be seen from Table II that the measured DD total yield shows a gradual increase with beam energy. Taking into account the error bars, the trend could be also constant. In both cases, the measured trend is different from the rise-and-fall behavior reported in Ref. [24] for the same CN but using a much more asymmetric reaction.

Unfortunately, because of the systematic experimental uncertainties owing to the energy loss, it was not possible to deduce the shape of the DD photon yield.

TABLE II. The values of the total DD yields for the reaction ^{16}O + ^{116}Sn at different beam energies.

Beam energy (MeV/nucleon)	DD total yield	Reference
8.1	$(3.6 \pm 1.9) \times 10^{-4}$	[18]
12	$(4.6 \pm 1.2) \times 10^{-4}$	This work
15.6	$(6.3 \pm 2.9) \times 10^{-4}$	[18]

V. THEORETICAL PREDICTIONS

To evaluate the amount of DD preequilibrium γ emission we used the BNV model, which describes the time evolution of the nuclear one-body density in phase space [8]. The DD emission is calculated applying the bremsstrahlung formalism in the evolution of the collective dipole oscillation from the beginning of the fusion process, when it arises, until it is completely damped to a pure "thermal" component, around 200 fm/c after the collision occurred [21]. In this way it is possible to calculate the whole contribution of the preequilibrium dipole radiation to the photon yield [6] in a consistent way.

The BNV equations were solved adopting the test particle method: Each nucleon was associated to a given number of test particles, to ensure a proper mapping of phase space. Each BNV simulation described a reaction event for the chosen projectile and target at fixed impact parameter and selected beam energy. The used parameters (10 events per impact parameter and 700 test particles) were chosen to minimize the numerical uncertainties associated with the computational technique using the available CPU power. In the code, the neutron-neutron and the proton-proton cross sections were parametrized as discussed in Ref. [43] and the neutron-proton cross section reported in Ref. [44] was used. These cross section parametrizations include in-medium effects and isospin, energy, and angle dependence. Two different symmetry terms of the EOS were compared. In particular, we used a "stiff" ($L_{\rm symm}$ = 72.6 MeV) and a "soft" ($L_{\rm symm}$ = 14.5 MeV) parametrization, where $L_{\rm symm}$ denoted the density derivative of the symmetry energy evaluated at normal density.

Calculations were performed for the reaction ^{16}O + ^{116}Sn at 8.1, 12, and 15.6 MeV/nucleon. The plot in Fig. 6 shows the calculated total DD yield for the two parametrizations of the symmetry term of the EOS as a function of different impact parameters. The curves, shown for a beam energy of 8.1 MeV/nucleon, have a very similar behavior independently

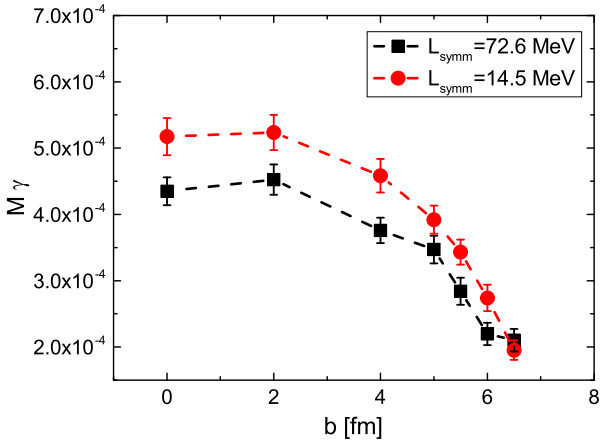

FIG. 6. (Color online) The calculated DD total yield for the reaction ^{16}O + ^{116}Sn at 8.1 MeV/nucleon as a function of the impact parameter. The black squares refer to the stiff case while red dots correspond to the soft parametrization of the symmetry term in the EOS.

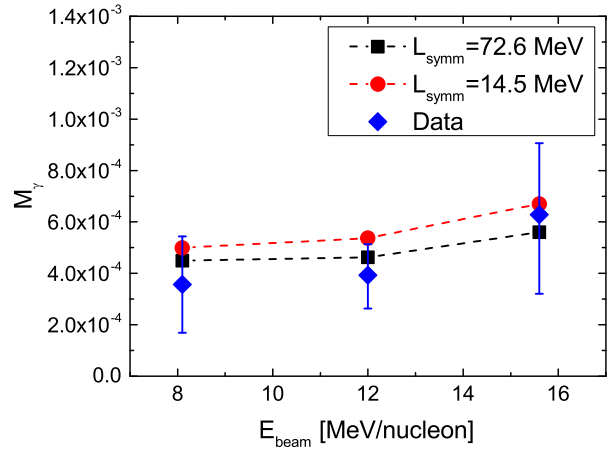

FIG. 7. (Color online) The DD yield as a function of the beam energy. The experimental data (blue diamonds) are compared to the theoretical predictions of the BNV model for the stiff (black squares) and the soft (red dots) parametrizations. The data at 8.1 and 15.6 MeV/nucleon are from Ref. [18].

on the beam energy and the reaction. The error bars come from the estimation of the numerical uncertainties in the calculations. It appears that for small impact parameters, there is a 20%–30% difference between stiff and soft predictions. For larger impact parameters the total yield decreases and the relative difference between stiff and soft predictions tends to decrease too. Figure 6 shows that it should be possible to observe a sensitivity to $L_{\rm symm}$ even using stable beams using DD data by selecting low spins, for example with a multiplicity filter (not present in the present experiment). It is important to notice that the difference between the DD total yield in a stiff or soft EOS scenario seems to be quite a general feature: Indeed, it was found in the calculations for all used reactions or beam energies.

All the calculations were performed in the impact parameter interval relevant for the fusion process, b = 0–6.5 fm. The results obtained for each impact parameter have been summed and weighted according to the cross section associated with CN formation. Note that a shift of 5$\hbar$ in the spin distribution introduces only a change less than 5% in the total yield, which falls within the error bar of our measurement. The results of the BNV simulations compared to the experimental data are shown in Fig. 7.

The plot shows that the BNV model predicts a weakly rising trend as a function of the beam energy similar to the one we found in the experimental data. Unfortunately, the error bars do not allow any conclusion about the stiff or soft nature of the EOS. It is, however, important to stress that the main contribution to the error bars does not come from either statistics or statistical model calculations but from the uncertainty in the estimation of the preequilibrium particle energy loss.

VI. ANGULAR DISTRIBUTION

From the experimental data it was also possible to extract the DD γ-ray angular distribution. This should have a dipole

shape but, owing to the rotation of the dipolar axis along the γ emission process, it is expected to be quenched with respect to a pure dipolar angular distribution. The angular distribution was obtained using the formula

$$W(\theta) \approx 1 + a_2 P_2(\cos\theta), \tag{3}$$

where P_2 is the Legendre polynomial $P_2(\cos\theta) = \frac{1}{2}[3\cos^2(\theta) - 1]$ and a_2 is a quenching factor.

To extract the angular distribution, we first normalized the response of the BaF_2 at different angles on the 15.1 MeV monochromatic emission produced in the reaction $^{11}B + d \Rightarrow {}^{12}C + n$. Before the extraction of the a_2 coefficient, the statistical contribution in the spectra was subtracted. It is important to remember that the measured angular distribution includes also the GDR angular anisotropy, which in this case is very small and both positive and negative [45,46]. From our data at 12 MeV/nucleon we measured a quenched angular distribution with an a_2 value of -0.36, as shown in Fig. 8. The obtained quenching factor a_2 turns out to be similar to the one measured for the $^{16}O + {}^{116}Sn$ reaction at 15.6 MeV/nucleon [18].

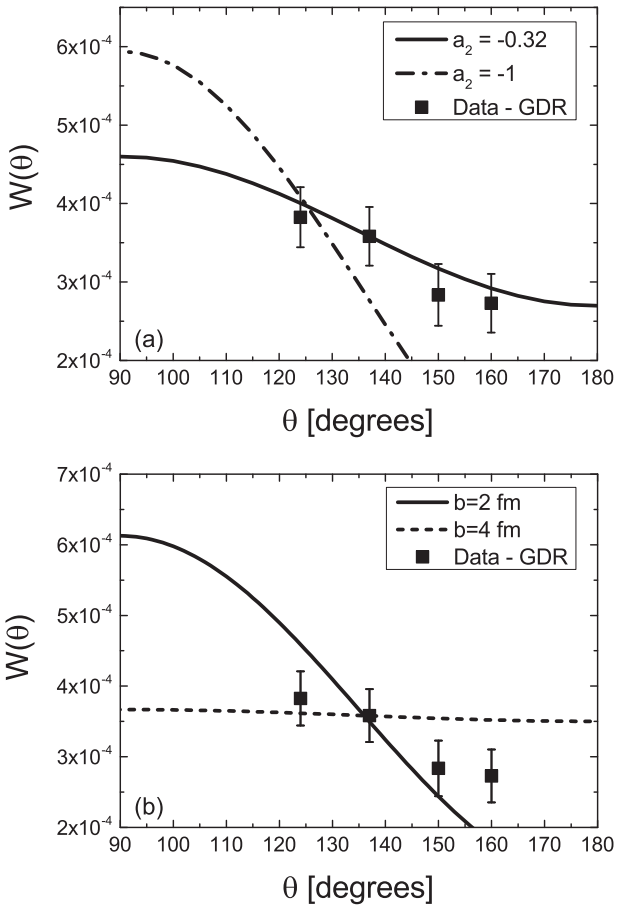

FIG. 8. (a) The measured DD γ emission angular distribution in the laboratory system (black squares). Data can be fitted by a dipole distribution quenched by a factor $a_2 = -0.36$ (black line). The theoretical model prediction for soft parametrization is shown as a dotted line and for the stiff one as a dashed line. The dot-dashed line represents a pure dipole angular distribution. (b) The measured DD angular distribution compared with the theoretical expectation, for impact parameter $b = 2$ and $b = 4$ fm, obtained in the soft case.

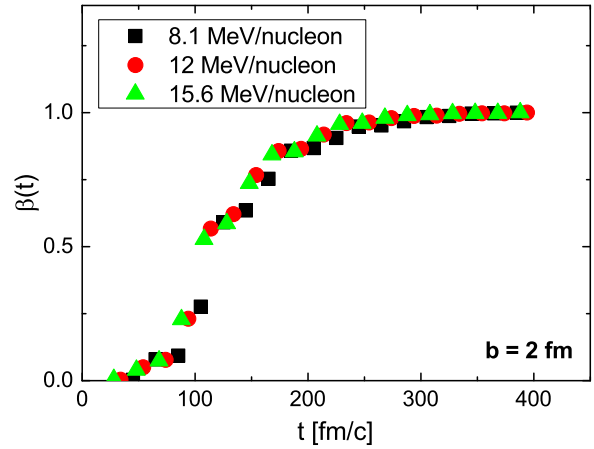

FIG. 9. (Color online) Integral emission probability $\beta(t)$ calculated at $b = 2$ fm for the three different beam energies for the stiff parametrization of the symmetry term of the EOS. The curves for the impact factors 0, 4, and 6 fm, not shown, are very similar.

The BNV model predicts a quenching factor much larger than the measured one. The model predicts that, during the fusion process, the nucleus emits DD γ rays while rotating and, therefore, different orientations of the dipole axis contribute to the angular distribution.

The difference between the measured quenching factor and the one obtained from the BNV model seems to suggest an instantaneous γ-ray emission which catches a snapshot of the dipole axis position while it is rotating. This hypothesis could also explain the measured angular distributions present in the literature [17,20]. A second possible origin of the discrepancy between the measured and calculated quenching factor a_2 could be associated with the weight attributed to each impact parameter in the calculations. In fact, even though the integral emission probability $\beta(t)$ (shown in Fig. 9 for the case $b = 2$ fm) has a very similar trend for different impact parameters, the corresponding $W(\theta)$ distributions are very different, as shown in the bottom panel of Fig. 8. A better agreement with data would be obtained attributing a lower weight to the large impact parameters ($b > 4$ fm).

Theoretical calculations including fission channels and producing a very detailed CN spin distribution for a fixed impact parameter are needed to properly weight the contribution to the measured γ angular distribution at different impact parameters.

VII. CONCLUSIONS

The DD emission in the reaction system $^{16}O + {}^{116}Sn$ at 12 MeV/nucleon was measured. This measurement, together with the ones at 8.1 and 15.6 MeV/nucleon of Ref. [18], provides the dependence of DD total yield on the projectile beam energy. These data are quite homogeneous: In fact, the reaction, the analysis technique and the experimental setup

are the same. Unlike the results reported in Ref. [24] in the case of a larger $D(0)$ value, we did not observe a rise-and-fall behavior, but a smooth increase of the DD yield as a function of the beam energy, in agreement with the BNV predictions. These results show that BNV approach seems to correctly describe the integral observables of the fusion dynamics at least in the case of small values of $D(0)$. Unfortunately, the experimental error bars do not allow any conclusion on the symmetry term of the EOS (L_{symm}). However, according to the theoretical BNV calculations, there should be a large difference in the DD total yield for different L_{symm} even using stable beams by selecting small impact parameters (low angular momenta). Therefore, this work suggests how it would be possible to test experimentally the symmetry term of the EOS using available stable beams.

The angular distribution was also measured and, even though a quenching was observed, as predicted by the BNV model, the experimental absolute value of a_2 turns out to be much larger than the theoretical one.

ACKNOWLEDGMENTS

The project is cofinanced by the European Union and the European Social Fund. This work was also supported by NuPNET-ERA-NET within the NuPNET GANAS project, under Grant Agreement No. 1 202914, and by the European Union, within the "7th Framework Program" FP7/2007-2013, under Grant Agreement No. 262010-ENSAR-INDESYS. The project it is also supported by Polish NCN Grant No. 2011/03/B/ST2/ 01894.

[1] C. Rizzo, V. Baran, M. Colonna, A. Corsi, and M. Di Toro, Phys. Rev. C **83**, 014604 (2011).
[2] M. B. Tsang, J. R. Stone, F. Camera, P. Danielewicz, S. Gandolfi, K. Hebeler, C. J. Horowitz, J. Lee, W. G. Lynch, Z. Kohley, R. Lemmon, P. Möller, T. Murakami, S. Riordan, X. Roca-Maza, F. Sammarruca, A. W. Steiner, I. Vidaña, and S. J. Yennello, Phys. Rev. C **86**, 015803 (2012).
[3] O. Wieland *et al.*, Phys. Rev. Lett. **102**, 092502 (2009).
[4] A. Carbone, G. Colò, A. Bracco, L. G. Cao, P. F. Bortignon, F. Camera, and O. Wieland, Phys. Rev. C **81**, 041301 (2010).
[5] J. M. Lattimer *et al.*, Phys. Rep. **442**, 109 (2007).
[6] V. Baran, C. Rizzo, M. Colonna, M. Di Toro, and D. Pierroutsakou, Phys. Rev. C **79**, 021603(R) (2009).
[7] Bao-An Li *et al.*, Phys. Rep. **464**, 113 (2008).
[8] V. Baran *et al.*, Phys. Rep. **410**, 335 (2005); V. Baran, Nucl. Phys. A **679**, 373 (2001).
[9] Ph. Chomaz *et al.*, Nucl. Phys. A **563**, 509 (1993).
[10] C. Simenel, Ph. Chomaz, and G. de France, Phys. Rev. Lett. **86**, 2971 (2001).
[11] C. Simenel, Ph. Chomaz, and G. de France, Phys. Rev. C **76**, 024609 (2007).
[12] P. F. Bortignon *et al.*, Nucl. Phys. A **583**, 101 (1995).
[13] S. Flibotte *et al.*, Phys. Rev. Lett. **77**, 1448 (1996).
[14] M. Cinausero *et al.*, Nuovo Cimento **111**, 613 (1998).
[15] D. Pierroutsakou *et al.*, Phys. Rev. C **71**, 054605 (2005).
[16] M. Papa *et al.*, Phys. Rev. C **72**, 064608 (2005).
[17] B. Martin *et al.*, Phys. Lett. B **664**, 47 (2008).
[18] A. Corsi *et al.*, Phys. Lett. B **679**, 197 (2009).
[19] C. Parascandolo *et al.*, Acta Phys. Pol. B **42**, 629 (2011); **44**, 605 (2013).
[20] C. Parascandolo *et al.*, Nucl. Phys. A **834**, 198c (2010).
[21] V. Baran, D. M. Brink, M. Colonna, and M. Di Toro, Phys. Rev. Lett. **87**, 182501 (2001).
[22] G. De Angelis *et al.*, J. Phys. Conf. Ser. **267**, 012003 (2011); web2.infn.it/spes/index.php/what-is-spes/tdr-2008.
[23] http://pro.ganil-spiral2.eu/spiral2/.
[24] D. Pierroutsakou *et al.*, Phys. Rev. C **80**, 024612 (2009).
[25] A. Maj *et al.*, Nucl. Phys. A **571**, 185 (1994).
[26] F. Gramegna *et al.*, Nucl. Instrum. Methods Phys. Res., Sect. A **389**, 474 (1997); M. Bruno *et al.*, Eur. Phys J. A **49**, 128 (2013).
[27] M. Bini *et al.*, Nucl. Instrum. Methods Phys. Res., Sect. A **515**, 497 (2003).
[28] L. Bardelli *et al.*, Nucl. Instrum. Methods Phys. Res., Sect. A **491**, 244 (2002).
[29] L. Bardelli *et al.*, Nucl. Instrum. Methods Phys. Res., Sect. A **572**, 882 (2007).
[30] J. Cabrera *et al.*, Phys. Rev. C **68**, 034613 (2003).
[31] M. P. Kelly, J. F. Liang, A. A. Sonzogni, K. A. Snover, J. P. S. van Schagen, and J. P. Lestone, Phys. Rev. C **56**, 3201 (1997).
[32] D. Prindle, R. Vandenbosch, S. Kailas, A. Charlop, and C. Hyde-Wright, Phys. Rev. C **48**, 291 (1993).
[33] K.A. Griffioen, E. A. Bakkum, P. Decowski, R. J. Meijer, and R. Kamermans, Phys. Rev. C **37**, 2502 (1988).
[34] V.L. Kravchuk, S. Barlini, and O. V. Fotina, Eur. Phys. J., EPJ Web Conf. **2**, 10006 (2010).
[35] D. Hilscher *et al.*, Phys. Rev. C **20**, 576 (1979).
[36] O. V. Fotina *et al.*, Int. J. Mod. Phys. E **19**, 1134 (2010).
[37] D. J. Hinde, D. Hilscher, H. Rossner, B. Gebauer, M. Lehmann, and M. Wilpert, Phys. Rev. C **45**, 1229 (1992).
[38] M. P. Kelly, K. A. Snover, J. P. S. van Schagen, M. Kicińska-Habior, and Z. Trznadel, Phys. Rev. Lett. **82**, 3404 (1999).
[39] O. Wieland *et al.*, Phys. Rev. Lett. **97**, 012501 (2006).
[40] W. Reisdorf, Z. Phys. A **300**, 227 (1981); A. V. Ignatyuk *et al.*, Sov. J. Nucl. Phys. **21**, 255 (1975).
[41] I. Diószegi, I. Mazumdar, N. P. Shaw, and P. Paul, Phys. Rev. C **63**, 047601 (2001).
[42] R. Brun *et al.*, CERN Report No. CERN-DD/EE/84-1, 1984.
[43] G. Q. Li and R. Machleidt, Phys. Rev. C **48**, 1702 (1993).
[44] G. Q. Li and R. Machleidt, Phys. Rev. C **49**, 566 (1994).
[45] K. Mazurek *et al.*, Acta Phys. Pol. B **38**, 1455 (2007), and references therein.
[46] K. Mazurek (private communication).